Journal of Catalysis **196,** 262–270 (2000)
doi:10.1006/jcat.2000.3041, available online at http://www.idealibrary.com on IDEAL®

Influence of Palladium Precursors on Structural Properties and Phenol Hydrogenation Characteristics of Supported Palladium Catalysts

Nagendranath Mahata[1] and V. Vishwanathan

Catalysis & Physical Chemistry Division, Indian Institute of Chemical Technology, Hyderabad 500 007, India

Received March 16, 2000; revised July 6, 2000; accepted August 22, 2000

$Pd(OOCCH_3)_2$, $PdCl_2$, and $Pd(NH_3)_4Cl_2$ were used to study the influence of palladium precursors on structural properties and phenol hydrogenation characteristics of Al_2O_3- and MgO-supported palladium catalysts. Palladium dispersion as well as phenol conversion is higher over MgO-based catalysts with the respective palladium precursors. $Pd(OOCCH_3)_2$ shows good metal dispersion and phenol hydrogenation activity over both of the supports. $Pd(NH_3)_4Cl_2$ leads to lower dispersion of Pd, probably due to the presence of inherent NH_3 (a reducing agent) and facile surface mobility of the precursor. The presence of chlorided Pd species in reduced Pd/Al_2O_3, originating from precursor $PdCl_2$, was confirmed by UV–visible spectroscopy. The initial activity of phenol hydrogenation is directly proportional to the palladium area over the catalysts prepared with $Pd(OOCCH_3)_2$ and $Pd(NH_3)_4Cl_2$; the activity shows a negative deviation over the catalysts originating from $PdCl_2$. Palladium precursors do not have a significant influence on the distribution of products. Al_2O_3-based catalysts are totally selective for cyclohexanone production, whereas MgO-based catalysts, along with cyclohexanone, produce cyclohexanol as the minor product. A comparison of the product distributions and the overall conversion of phenol over the MgO-based catalysts reveals that changes in product selectivity cannot be attributed merely to a change in the conversion level and also that one product does not form at the expense of another. Al_2O_3-based catalysts show initial deactivation, while MgO-based catalysts show strong resistance to deactivation. © 2000 Academic Press

Key Words: **palladium precursor; supported palladium; residual chlorine; phenol hydrogenation; structure–activity relationship.**

1. INTRODUCTION

Palladium occupies a special place among those transition metals that are commonly used as heterogeneous catalysts. An excellent review of palladium catalysts was presented by Karpinski (1). Catalysis on supported, unsupported, and electron-deficient palladium and structure–activity correlations with some specific examples are covered in that review. Even though chemists generally recognize the versatility of palladium in hydrogenation reactions, an explanation of its "magic" catalytic properties, however, is still far from being satisfactory (2). The catalytic behavior of a supported metal depends strongly on the variables involved in preparation and pretreatment. The metal precursor is such a variable. In a supported metal catalyst, dispersion of the metal depends strongly on the precursor–support interaction as well as on the size of the precursor. A fragment of a precursor attached to the active component (e.g., Cl^- in the case of chloride salt as precursor), being residual after pretreatment, can also influence the properties of the catalyst support and/or of the active component. To be precise, the precursor plays a considerable role in shaping the properties of the final catalyst. In recent years there have been a number of attempts to solve the problem of preparing palladium catalysts using different precursors (3–12), but the chemistry of the precalcination–reduction steps is still not fully understood. For example, it is known that residual chlorine from chlorinated precursor has an effect on the catalytic properties (7, 10–18). However, the exact state and role of residual chlorine are not fully understood. Ali and Goodwin (10) used $PdCl_2$ and $Pd(NO_3)_2$ as precursors for supported Pd catalysts to study CO hydrogenation; the precursor did not seem to affect Pd dispersion. However, they found that $PdCl_2$-based catalysts were more active than $Pd(NO_3)_2$-based catalysts. Sepulveda and Figoli (11), in their study of styrene hydrogenation over supported Pd catalysts originating from amine complexes of $PdCl_2$, $Pd(NO_3)_2$, and $Pd(Ac)_2$, observed a clearly toxic effect of residual chlorine. However, they did not determine whether the chlorine is in the Pd particles. Sales *et al.* (12) observed chlorinated Pd species in a $PdCl_4^{2-}$-based Pd–Sn/Al_2O_3 catalyst, even after calcination in air at 773 K. However, no study has been made of the sample after reduction. Bozon-Verduraz *et al.* (18) made XPS measurements which revealed the presence of surface complexes, involving palladium and chlorine, in reduced supported Pd catalysts. However, they omitted the usual calcination step in the pretreatment sequence. Further studies are required

---

[1] To whom correspondence should be addressed. Present address: 2.31, Institute of Chemistry, Chemical Research Center, Hungarian Academy of Sciences, P.O. Box 17, 1525 Budapest, Hungary. E-mail: nmahata@cric.chemres.hu.

0021-9517/00 $35.00

to understand the exact state and role of residual chlorine. Comparative studies using inorganic and organic salts of palladium as precursors are also limited. Our study is concerned with the attempts to find solutions to the above-mentioned problems.

The vapor-phase hydrogenation of phenol to cyclohexanone is an important industrial reaction for the production of caprolactam, a monomer used in making Nylon-6. Cyclohexanone is produced catalytically either by oxidation of cyclohexane or by hydrogenation of phenol. Oxidation of cyclohexane on a large scale requires high temperature and pressure. It is very likely that the process will lead to other undesirable oxidation products. This in turn would lower the product yield and complicate the recovery and purification stages. In the hydrogenation of phenol, cyclohexanone can be generated in a one- or two-step process. In the latter case, phenol is first hydrogenated to cyclohexanol, and that is then dehydrogenated, in the second step, to cyclohexanone. Replacing the two-step process by a single step is advantageous, because it eliminates the cyclohexanol dehydrogenation step, which is highly endothermic. The importance of the reaction is reflected in the number of patents and publications devoted to it (19–40). The reaction has been studied over a range of palladium-based (22–33) and platinum-based (27, 34–38) catalysts. There are also reports of the reaction over rhodium (36) and nickel (39, 40) catalysts. The influence of process variables such as reaction temperature (24, 27–30, 32, 36, 39), time (23–25, 28–30), and concentration of the reactant(s) (23–30, 32, 39) on activity/selectivity has been documented, and kinetic aspects have been considered in a number of publications (25, 26, 28–32, 36–39). Studies have also been conducted on metal loading (23, 25, 28–30, 40), promoters (24, 25, 29, 33), and alloying with a second metal (34, 35). However, there is, to date, a lack of comprehensive studies on the reaction over catalysts that originate from different metal precursors. There is also a lack of studies on the structure–activity relationship, and some of the existing reports are contradictory. While some reports indicate that an acidic support is beneficial for cyclohexanone formation (24, 25, 27), others indicate that a basic support is beneficial (28, 29). Chen *et al.* (28) observed again that the reaction is structure-sensitive, whereas according to Galvagno *et al.* (30) it is structure-insensitive over supported palladium catalysts. Further studies are required to settle these controversies. In the present study, an acidic (Al_2O_3) and a basic (MgO) support as well as three different palladium precursors, ($Pd(OOCCH_3)_2$, $PdCl_2$, and $Pd(NH_3)_4Cl_2$), were investigated to determine the possible effects of the supports and the effects of the metal precursors on the structural properties and the phenol hydrogenation characteristics of supported palladium catalysts. An attempt has also been made to adopt a structure–activity relationship.

2. EXPERIMENTAL

2.1. Catalyst Preparation

Pd/Al_2O_3 and Pd/MgO catalysts (1 wt% Pd loading) were prepared using $Pd(OOCCH_3)_2$ (Aldrich), $PdCl_2$ (Loba-Chemie), and $Pd(NH_3)_4Cl_2$ (prepared from a $PdCl_2$ solution) as metal precursors, employing the marginally excess volume wetness impregnation method. About 5 g of the carriers (γ-Al_2O_3 (Harshaw), $SA = 234\ m^2\,g^{-1}$; MgO (Marfina Marietta), $SA = 45\ m^2\,g^{-1}$) was added to the calculated amount of metal precursor solutions and stirred continuously. $Pd(OOCCH_3)_2$ was dissolved in CH_3CN, while $PdCl_2$ was used as an aqueous solution (mildly acidified with HCl, pH 3) (7, 12, 17, 26, 28–30, 32). A $Pd(NH_3)_4Cl_2$ solution was prepared by reacting a solution of $PdCl_2$ with concentrated NH_3 at 348 K and then diluting it with water (41). The suspensions were left for 2 h and stirred periodically. In the case of $Pd(OOCCH_3)_2$, the solvent CH_3CN was evaporated in a current of hot air, while in the other cases the solvent water was evaporated over a boiling water bath. The residues were dried overnight at 393 K in an air oven. The catalysts were subsequently calcined in air at 673 K for 4 h. The Pd/Al_2O_3 catalysts were referred to as **A**, **B**, and **C** (Table 1), while Pd/MgO catalysts were referred to as **I**, **II**, and **III** (Table 2) and were prepared using $Pd(OOCCH_3)_2$, $PdCl_2$, and $Pd(NH_3)_4Cl_2$ precursors, respectively.

2.2. UV–Visible Spectroscopy

UV–visible spectroscopy was used to detect chlorided Pd species in the reduced catalysts prepared using $PdCl_2$ and $Pd(NH_3)_4Cl_2$ as metal precursors. The catalysts were reduced in a flow of H_2 ($\sim$60 ml min^{-1}) at 573 K for 3 h and then brought to room temperature in a flow of H_2. The reduced catalysts were extracted with hot water. The catalysts were added to water and ground, and the mixtures were boiled. The contents were filtered and the filtrates were centrifuged (15,000 rpm). The transparent supernatant liquids were examined by means of a Beckman DU-7000 UV–visible spectrophotometer. The idea behind this was that, if residual chlorine is associated with palladium, or in other

TABLE 1

CO Adsorption Characteristics of 1 wt% Pd/Al_2O_3 Catalysts Prepared from Different Palladium Precursors

Pd precursor	CO_{irr} uptake (μmol g^{-1} cat)	Dispersion, *D*	Metal area (m^2)		Particle size, *d* (nm)
			g^{-1} cat	g^{-1} Pd	
$Pd(OOCCH_3)_2$ (**A**)	45.3	0.48	2.15	215	2.3
$PdCl_2$ (**B**)	37.1	0.39	1.76	176	2.9
$Pd(NH_3)_4Cl_2$ (**C**)	21.5	0.23	1.02	102	4.9

TABLE 2

CO Adsorption Characteristics of 1 wt% Pd/MgO Catalysts Prepared from Different Palladium Precursors

Pd precursor	CO_{irr} uptake (μmol g^{-1} cat)	Dispersion, D	Metal area (m^2)		Particle size, d (nm)
			g^{-1} cat	g^{-1} Pd	
$Pd(OOCCH_3)_2$ (**I**)	52.6	0.56	2.50	250	2.0
$PdCl_2$ (**II**)	47.7	0.51	2.26	226	2.2
$Pd(NH_3)_4Cl_2$ (**III**)	35.0	0.37	1.66	166	3.0

words if chlorided Pd species are still present even after reduction, then water would extract them as aquo species ($PdCl_x(H_2O)_{4-x}$; $1 \leq x \leq 4$), which would be detected by UV–visible spectroscopy.

2.3. *Chemisorption Measurements*

CO chemisorption measurements were carried out at room temperature using a conventional, glass, high-vacuum volumetric apparatus. In a typical experiment, the catalyst was reduced in a flow of H_2 ($\sim$60 ml min^{-1}) at 573 K for 3 h and evacuated to 10^{-6} Torr (1 Torr = 133.3 N m^{-2}) at the same temperature for 3 h. The catalyst was brought to room temperature under vacuum. After introduction of CO to the sample tube containing the catalyst, the total and the reversible isotherms were evaluated. After the first isotherm, i.e., total CO uptake, was measured, the sample was evacuated for 30 min at room temperature, and then the second isotherm, i.e., the reversible CO uptake was measured. Using the difference between the total and the reversible chemisorbed CO, the number of exposed Pd metal atoms was calculated, assuming a chemisorption stoichiometry of CO/Pd = 1 (10, 12, 30, 42–45). Hence, the number of exposed Pd atoms per gram of catalyst on the surface, N_s, is equal to the number of CO molecules that were irreversibly chemisorbed, i.e., CO_{irr} uptake per gram of catalyst.

Dispersion (D), i.e., the fraction of exposed Pd, is given by $D = N_s/N_t$, where N_t is the total number of Pd atoms per gram of catalyst. The area and particle size of the metal were calculated according to the procedures described by Anderson (46). The total metal surface area, A, is given by $A = (N_s/1.27 \times 10^{19})$ $m^2\,g^{-1}$ catalyst, where 1.27×10^{19} is the number of surface atoms per square meter of the polycrystalline palladium surface (46).

Volume–area mean particle diameter, d, is given by $d = 6(v_M/a_M)/D$, where a_M and v_M are the effective average area occupied by a palladium atom in the surface and the volume per metal atom in the bulk, respectively (46). D is the dispersion. Now, $v_M = (M_w/\rho N_o)$ m^3, where M_w is the atomic weight, ρ the density (expressed in g m^{-3}), and N_o Avogadro's number, while $a_M = (1/1.27 \times 10^{19})$ m^2. Hence, using the values of M_w, ρ, and N_o,

$$d = (1.12/D) \times 10^{-9}\ \text{m} = (1.12/D)\ \text{nm}.$$

The CO chemisorption capacity of the pure supports (Al_2O_3 and MgO) was also checked after the same pretreatment as for the catalysts.

NH_3 chemisorption measurements were made at room temperature using the same volumetric apparatus as used for the CO chemisorption measurements. Before the measurement, the samples were pretreated at 423 K for 2 h under vacuum.

2.4. *Hydrogenation of Phenol*

The catalysts were evaluated for vapor-phase hydrogenation of phenol in a vertical fixed-bed, continuous down-flow glass microreactor at 503 K under ambient pressure. In a typical experiment, 0.5 g of catalyst (40–60 mesh, bed length $\sim$3 mm) was packed between the layers of quartz wool, and the upper portion of the reactor was filled with glass beads, which served as preheaters for the reactants. The catalyst was reduced in a flow of hydrogen ($\sim$60 ml min^{-1}) at 573 K for 3 h and brought to the reaction temperature. Due to the difficulty of the operation with pure phenol, it was dissolved in cyclohexane (1 : 2 w/w) and fed into the reactor at a calculated rate from the top of the reactor using a calibrated motorized syringe (B. Braun). The reaction occurred in the flow integral mode. The H_2/phenol molar ratio, the flow rate of phenol, and the weight of the catalyst were maintained at 5.4, 0.0135 mol h^{-1}, and 0.5 g, respectively, and kept constant in all experiments. Since the grain size of the catalyst was large enough and the bed sufficiently short, it was assumed that there were no limitations to mass/heat transfer. However, the present study is not devoted to the kinetic aspect. The reaction products were analyzed using a gas chromatograph (CIC) equipped with a Carbowax 20M on a Chromosorb W column and a flame ionization detector (FID).

3. RESULTS AND DISCUSSION

3.1. *UV–Visible Spectroscopy*

As mentioned in the Introduction, chlorine remains on the catalyst even after pretreatment when chlorinated precursors are used to prepare the supported Pd catalyst. A qualitative $AgNO_3$ test with the water extracts of the reduced catalysts (**B**, **C**, **II**, and **III**), originating from chlorinated precursors ($PdCl_2$ or $Pd(NH_3)_4Cl_2$), confirmed the presence of residual chlorine on the catalysts surface. However, this test cannot reveal whether the chlorine resides on metal particles or on the support. It is important to know whether Pd particles contain any residual chlorine or, in other words, whether chlorided palladium species are still present even after reduction. The aim of the present study was not to quantify the residual chlorine in metal particles but to make a qualitative search for it and to reveal its possible influence on catalytic activity. Future work is planned on the quantification of residual chlorine associated with metal particles. Palladium particles usually become chlorine-free during pretreatment (drying–reduction), but a small amount of chlorine may remain associated. An XPS study by Bozon-Verduraz *et al.* (18) revealed the presence of a palladium–chlorine surface complex in a reduced, supported Pd catalyst derived from $PdCl_2$. However, those authors directly reduced the dried catalysts, avoiding the usual calcination step during pretreatment. A TOF–SIMS study by Zhou *et al.* (47) confirmed the presence of Cl atoms bound to Pt after high-temperature oxidation and reduction of the Pt/Al_2O_3 catalyst that originated from H_2PtCl_6. Johnston and Joyner (48) used EXAFS which revealed Rh–Cl bonding in the reduced Rh/Al_2O_3 catalyst prepared from $RhCl_3$. In the present study, a very simple and widely available technique, UV–visible spectroscopy, was used to check whether Pd particles contain residual chlorine. Water extracts of the reduced catalysts (**B**, **C**, **II**, and **III**), originating from chlorinated precursors (either $PdCl_2$ or $Pd(NH_3)_4Cl_2$), were examined for chlorided Pd species using the same technique. Figure 1 shows the UV–visible spectra of the water extract of the reduced catalyst **B** along with the blank solution (distilled water). An absorbance band around 270 nm can be seen clearly. Furthermore, careful observation reveals the shoulders around 280, 315, and 400 nm. An absorbance band around 270 nm ($\lambda^{-1} = 3.7\ \mu m^{-1}$) can be assigned to the combined contribution of $PdCl(H_2O)_3^+$ and $PdCl_4^{2-}$ species (49), whereas the shoulders around 280 nm ($\lambda^{-1} = 3.57\ \mu m^{-1}$), 315 nm ($\lambda^{-1} = 3.17\ \mu m^{-1}$), and 400 nm ($\lambda^{-1} = 2.5\ \mu m^{-1}$) can be assigned to $PdCl_4^{2-}$, $PdCl_3(H_2O)^-$, and $PdCl(H_2O)_3^+$ species, respectively (18, 49). Of the species observed, $PdCl(H_2O)_3^+$ probably dominates. The presence of chlorided Pd species in reduced catalyst **B** was not unexpected. It is very difficult to convert all of the $PdCl_2$ to PdO in air at 673 K, which is the temperature at which calcination took place in this study. It was reported that $PdCl_2$ supported on zeolite (NaX) can be converted completely to PdO at or above 773 K in an oxygen atmosphere (50). A fraction of $PdCl_2$, which was present after calcination, is likely to remain associated with the metal particles even after hydrogen treatment (18, 47, 48). Spectra (not shown) of the water extracts of the other three catalysts (**C**, **II**, and **III**), originating from chlorinated precursors, were similar to that of the blank. The absence of chlorided Pd species in the water extract of the reduced catalysts **C** and **III** (originating from $Pd(NH_3)_4Cl_2$) is not surprising. During precalcination, the inherent reducing agent NH_3 may reduce Pd^{2+} to Pd^0, forming HCl, and the HCl produced was immediately consumed by one extra NH_3 molecule. In catalyst **III**, the HCl produced was consumed by magnesia in addition to NH_3. The other possibility is that NH_3 takes away Cl^- along with surface H^+, forming NH_4Cl during the decomposition of $Pd(NH_3)_4Cl_2$. Any trace amount of chlorine, associated with palladium after drying and calcination, is removed during reduction. It is interesting that no residual chlorine is present in palladium particles on the MgO support that originates from $PdCl_2$ (catalyst **II**). One explanation might be that basic MgO facilitates the complete reduction of palladium. When water extracted from the calcined Pd/MgO, treated in the same way as for the reduced catalysts, was examined, no chlorided Pd species were found. This shows that $PdCl_2$ over MgO completely decomposes during or even before calcination. It is unlikely that $PdCl_2$ decomposes completely during calcination over MgO but not over Al_2O_3. The situation may be explained as follows: during impregnation, MgO reacts with water to form strong alkali $Mg(OH)_2$ as

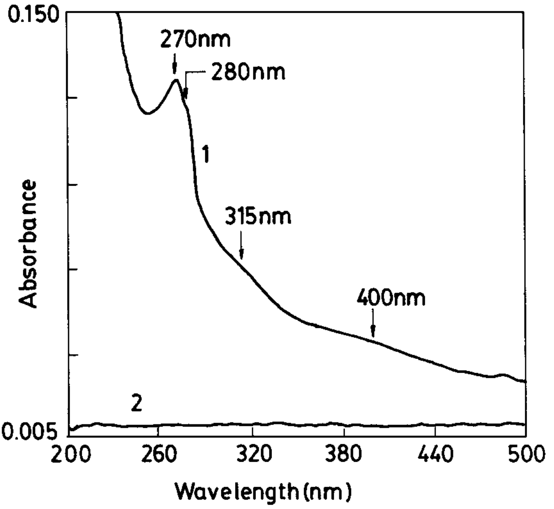

FIG. 1. UV–visible spectra of (1) water extract of reduced catalyst **B** (1 wt% Pd/Al_2O_3, prepared using $PdCl_2$) and (2) blank solution (distilled water).

$$MgO + H_2O = Mg(OH)_2.$$

According to Sales *et al.* (12), a basic OH^- group can be exchanged by the Cl^- of $PdCl_2$. Thus, during impregnation and calcination, $PdCl_2$ reacts with $Mg(OH)_2$ to give $Pd(OH)_2$ as

$$PdCl_2 + Mg(OH)_2 = Pd(OH)_2 + MgCl_2.$$

The capacity of MgO to form strong alkali $Mg(OH)_2$ by reacting with water (51) means that it could react as described above. Jiang *et al.* (52) also proposed a model for the solid-state exchange reaction between MgO and transition metal chloride to form $MgCl_2$ and transition metal oxide. Even though the Pd particles are free of Cl, a considerable amount of Cl probably remains at the interface of the metal support in the form of $MgCl_2$.

The above mechanism may also be involved in removing some of the chlorine from the palladium in the Pd/Al_2O_3

catalyst, originating from $PdCl_2$ (12). This is because at least a small amount of Al_2O_3 is likely to react with water to form $Al(OH)_3$ (amphoteric hydroxide) near the surface (51).

3.2. CO Chemisorption

Exposed areas of palladium of the catalysts were calculated from the irreversible CO chemisorption measurement (10, 12, 30, 42–45). Irreversible CO chemisorption over the supports (Al_2O_3 and MgO) was found not to occur. Hence, it is clear that there was no contribution from the supports in the irreversible CO chemisorption of the catalysts. However, some reports state that MgO can strongly chemisorb CO after pretreatment under severe conditions ($T \geq 1000$ K, vacuum) (53, 54). In the present study, pretreatment was done under comparatively mild conditions ($T = 573$ K, H_2 flow; subsequent evacuation at the same temperature) before the CO chemisorption measurement was made. That may explain the absence of irreversible CO chemisorption over MgO in the present study. Galvagno *et al.* used CO chemisorption to characterize Pd/MgO catalysts and found consistent results (30).

Table 1 shows CO_{irr} adsorption characteristics of the Al_2O_3-based catalysts. Dispersion, i.e., the fraction of exposed palladium in the catalysts, follows the order **A** > **B** > **C**. The reason for the minimal dispersion of palladium in catalyst **C** may be the inherent presence of ammonia, a well-known reducing agent. During drying and/or calcination, "autoreduction" of $Pd(NH_3)_4^{2+}$ to Pd^0 takes place, and the primary clusters tend to agglomerate to large entities (55). However, other possibilities should also be considered. Partial decomposition of $Pd(NH_3)_4^{2+}$ produces $Pd(NH_3)_x^{2+}$ along with N_2 and H_2O (9, 56), and the H_2O produced is likely to facilitate the agglomeration of $Pd(NH_3)_x^{2+}$, which leads to lower metal dispersion (4). High surface mobility of the precursor may also lead to lower dispersion of palladium (3). The difference in palladium dispersion between catalysts **A** and **B** can be explained as follows: $Pd(OOCCH_3)_2$ easily converts to PdO during calcination, and the oxide–oxide interaction causes it to spread uniformly over Al_2O_3. The easily reducible PdO results in higher metal dispersion, whereas the presence of residual chlorine in the Pd particles of catalyst **B** results in a comparatively lower uptake of the probe gas and, hence, lower dispersion of palladium (57). Agglomeration of partially decomposed $PdCl_2$ during reduction may also take place, resulting in lower metal dispersion in catalyst **B** (58). Another possibility may be the difference in size between the counteranions. The CH_3COO^- is much larger than Cl^-, and hence CH_3COO^- ions keep the Pd^{2+} ions apart in contrast to Cl^-. Consequently, smaller PdO particles form during calcination, and subsequent reduction results in greater dispersion of palladium when the precursor is $Pd(OOCCH_3)_2$ (30). It is possible that carbonaceous residue reduces the uptake of the probe gas by blocking some Pd sites, which should be reflected in the lower dispersion of palladium when the precursor is $Pd(OOCCH_3)_2$. However, the calcination temperature in this study is high enough (673 K) to decompose the acetate groups completely and to remove all of the carbon. Lomot *et al.* (9) reported that 523 K is sufficient to remove all the carbon from $Pd(acac)_2/SiO_2$, even with 1% O_2 in an He atmosphere.

The characteristics of CO adsorption of the MgO-based catalysts are shown in Table 2. Dispersion of palladium varies in the order **I** > **II** > **III**. Similar to the Al_2O_3-based catalysts, the low dispersion of palladium in catalyst **III** (originating from $Pd(NH_3)_4Cl_2$) can account for facile surface mobility and "autoreduction" of the precursor (3, 55). However, the water-assisted agglomeration of the partially decomposed precursor probably does not occur. MgO probably consumes the liberated H_2O readily (51) during the decomposition of $Pd(NH_3)_4^{2+}$. Similar to the Al_2O_3-based catalysts, the slightly higher dispersion of Pd in catalyst **I** (derived from $Pd(OOCCH_3)_2$) compared to catalyst **II** (derived from $PdCl_2$) can be attributed to the larger size of the counteranion (30). However, the agglomeration of the precursor during reduction and residual chlorine-induced lowering of CO chemisorption probably does not occur. Catalyst **II** does not contain any chlorided Pd species after calcination, as shown by UV–visible spectroscopy (Section 3.1).

A comparison of Pd/Al_2O_3 and Pd/MgO catalysts reveals that MgO-based catalysts show higher Pd dispersion compared to Al_2O_3-based catalysts with the respective metal precursors, even though the BET surface area of Al_2O_3 (234 $m^2\ g^{-1}$) is much greater than that of MgO (45 $m^2\ g^{-1}$). The impact of the BET surface area of the supports is likely to be minimal or nonexistant, because the loading of the metal is low enough (1 wt%). The specific area of Pd (per gram of catalyst) is much lower (1 to 2.5 m^2; Tables 1 and 2) than the BET surface area of the supports. Higher dispersion of Pd over MgO may be due to the stronger interaction of Pd with basic MgO compared to acidic/amphoteric Al_2O_3. Lopez and Illas (59) investigated the nature of the interaction of Pd with the acidic and basic sites of the MgO(100) surface by means of ab initio wave functions and DFT techniques. They predicted a fairly strong interaction of Pd over basic sites but a rather weak interaction of the metal over acidic sites. A quantum chemical study by Ferrari and Pacchioni (60) also predicts a good interaction between Pd and MgO. The particle size of palladium in all of the catalysts, with all three Pd precursors and over both supports, is between 2 to 5 nm.

3.3. Phenol Hydrogenation

Figure 2 shows the plot of initial phenol hydrogenation activity versus the metal area of Pd/Al_2O_3 and Pd/MgO catalysts prepared from different Pd precursors. The initial activities were calculated from the conversion during

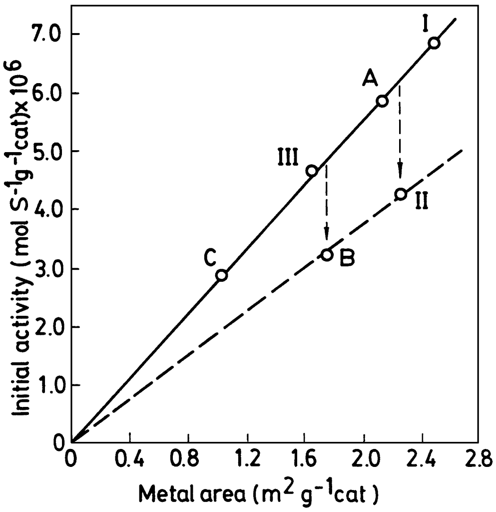

FIG. 2. Metal area versus initial phenol hydrogenation activity over 1 wt% Pd/Al_2O_3 (**A**, **B**, and **C**) and 1 wt% Pd/MgO (**I**, **II**, and **III**) catalysts prepared from three different Pd precursors: (**A** and **I**) $Pd(OOCCH_3)_2$; (**B** and **II**) $PdCl_2$; and (**C** and **III**) $Pd(NH_3)_4Cl_2$. Reaction conditions: $T = 503$ K; H_2/phenol mole ratio = 5.4; flow rate of phenol = 0.0135 mol h^{-1}; catalyst weight = 0.5 g.

the first 3 min of the reaction run using the formula xF/W, where x is fractional conversion, F the flow rate of phenol, and W the weight of catalyst. F and W were always constant. The activities of catalysts **A**, **C**, **I**, and **III** (derived from $Pd(OOCCH_3)_2$ and $Pd(NH_3)_4Cl_2$) are on a straight line that passes through the origin. However, catalysts **B** and **II** (derived from $PdCl_2$) show large negative deviations. Again, the activities of **B** and **II** fall on another straight line that passes through the origin. Hence, the activity is a direct function of the metal area. The proportionate negative deviations in the activities of catalysts **B** and **II**, compared to the other catalysts, lead to the speculation that the same or similar factors are responsible for it. The only factor that the two catalysts have in common is that both were prepared using a chloride precursor ($PdCl_2$). Examination with UV–visible spectroscopy confirmed the presence of residual chlorine associated with metal particles in catalyst **B**. However, metal particles in catalyst **II** are free of chlorine, as shown by the same technique. Even though residual chlorine is absent in Pd particles in catalyst **II**, it may still be present at the metal–support interface in the form of $MgCl_2$. The local environment of Pd may, at least to some extent, be made up of $MgCl_2$ and MgO. The presence of electronegative chlorine in Pd particles or at the metal–support interface may reduce the density of the electrons over palladium. Consequently, less electron transfer from Pd to the π^* antibonding orbital of the aromatic ring of chemisorbed phenol causes the activity of the aromatic ring to decrease. Thus, the activities of catalysts **B** and **II** show negative deviations. The presence of residual chlorine on or around metal particles may affect the hydrogen activation, too (61).

The performances of the catalysts in terms of phenol conversion, product selectivity, and turnover frequency (TOF) are shown in Table 3. TOFs over $Pd(OOCCH_3)_2$- and $Pd(NH_3)_4Cl_2$-based catalysts are the same, while they are considerably lower over $PdCl_2$-based catalysts, irrespective of the support. The presence of residual chlorine on or around metal particles is thought to be responsible for the lower TOF over the $PdCl_2$-based catalysts. The constancy of TOF, irrespective of the support, suggests that the support may not have a significant influence on the intrinsic activity of palladium in phenol hydrogenation. Higher phenol conversions over MgO-based catalysts are due to a larger available metal area. Again, direct proportionality between activity and metal area (as already shown in Fig. 2), which simply reflects the stability of TOF with changing metal particle sizes (as revealed by a direct comparison of Table 3 with Tables 1 and 2), makes it clear that the reaction is structure-insensitive over the supported Pd catalyst (30). The TOFs over the two $PdCl_2$-based catalysts are lower but similar and have already been discussed. However, Chen *et al.* (28) observed structure sensitivity with the hydrotalcite-supported Pd catalyst of varying metal loading. Irrespective of the precursor, Al_2O_3-based catalysts are almost totally selective for cyclohexanone production (23, 28, 34, 35), whereas MgO-based catalysts show 80 to 90% cyclohexanone and 10 to 20% cyclohexanol selectivity. No other byproducts were observed. The present study clearly shows that support materials play a clear role in the selectivity of the products of phenol hydrogenation over supported Pd catalysts. The acidic support favors cyclohexanone selectivity, while the basic support also induces cyclohexanol formation (24, 25, 27). The formation of cyclohexanol over MgO-based catalysts, which can be attributed to the strong basicity of the support, will be discussed below. However, Chen *et al.* (28) and Neri *et al.* (29) proposed

TABLE 3

Comparative Catalytic Performance of 1 wt% Pd/Al_2O_3 and 1 wt% Pd/MgO Catalysts Derived from Different Palladium Precursors

Pd precursor	Catalyst	Initial phenol conversion (%)	Product selectivity (%) CHN	CHL	TOF[a]
$Pd(OOCCH_3)_2$	Pd/Al_2O_3 (**A**)	77	98	02	0.13
	Pd/MgO (**I**)	90	82	18	0.13
$PdCl_2$	Pd/Al_2O_3 (**B**)	41	100	—	0.08
	Pd/MgO (**II**)	56	87	13	0.09
$Pd(NH_3)_4Cl_2$	Pd/Al_2O_3 (**C**)	37	100	—	0.13
	Pd/MgO (**III**)	61	86	14	0.13

[a] Number of phenol molecules converted per surface Pd atom per second. CHN = cyclohexanone; CHL = cyclohexanol. Reaction conditions: temperature = 503 K; H_2/phenol mole ratio = 5.4; flow rate of phenol = 0.0135 mol h^{-1}; catalyst weight = 0.5 g.

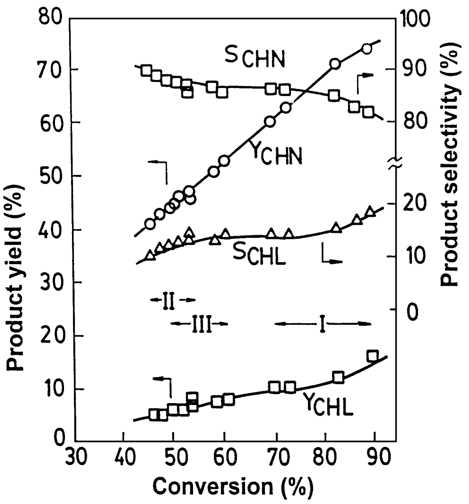

FIG. 3. Product yield (*Y*) and selectivity (*S*) as functions of phenol conversion over 1 wt% Pd/MgO catalysts prepared from three different Pd precursors: (**I**) $Pd(OOCCH_3)_2$; (**II**) $PdCl_2$; and (**III**) $Pd(NH_3)_4Cl_2$. Catalyst codes indicate the regions of conversion. CHN = cyclohexanone; CHL = cyclohexanol. Reaction conditions: see Fig. 2.

that the basicity of a support favors cyclohexanone production.

Product distribution over the MgO-based catalysts is shown as a function of conversion in Fig. 3. The yield and selectivity of each product were plotted against overall phenol conversion. The data presented in the figure were collected from time-on-stream experiments. Catalyst deactivation does not influence the product selectivity, as shown by the time-on-stream experiment over Pd/Al_2O_3 catalysts which become severely deactivated with time (as will be shown below), but product selectivity remains constant throughout the runs. Hence, product yield/selectivity, presented in Fig. 3, is a function of conversion. It is noteworthy that, irrespective of the Pd precursor, the respective points fall on smooth curves. This suggests that metal precursors do not have a strong effect on product distribution. The stability of product selectivity over a wide range of conversion (55 to 80%) indicates that a change in product selectivity may not be due to merely a change in phenol conversion. The decrease in cyclohexanone selectivity, accompanied by a simultaneous increase in cyclohexanol selectivity with increasing conversion (in the lower and higher regions of conversion), seems to show that cyclohexanol is formed at the expense of cyclohexanone. However, the correlation between product yield and conversion (as shown in the same figure) reveals the actual situation. The yields of both cyclohexanone and cyclohexanol increase linearly with increasing phenol conversion, though slight deviations are observed at very high conversion. An increase in the cyclohexanone yield is much more pronounced than that in the cyclohexanol yield in the conversion region. It is obvious that cyclohexanol does not form at the expense of cyclohexanone over the catalysts in this study. This and previous studies (36, 38, 39) suggest that product selectivity in the catalytic hydrogenation of phenol strongly depends on the active metal employed. However, acid/base properties of a support may have some influence (24, 25, 27–29). It is likely that cyclohexanone is the intermediate and cyclohexanol the final product over Pt and Ni catalysts (36, 38, 39), whereas the possibility that cyclohexanone is an intermediate over Rh catalyst has been ruled out (36). Our study suggests that cyclohexanone and cyclohexanol form independently via the intermediate cyclohexenol over the Pd catalyst. The desorption of cyclohexenol followed by subsequent rapid tautomerization leads to cyclohexanone formation. The high basicity of the surface induces cyclohexanol formation, too. Over the Pd/MgO catalysts, a fraction of strongly bound phenol (due to the strong basicity of MgO) in the form of phenolate, subsequently "en-olate," undergoes complete hydrogenation before desorption.

To examine the stability of the catalysts, they were tested for 8 h on stream. Figure 4 shows the deactivation profile of the Al_2O_3-based catalysts. After considerable deactivation, the catalysts attained steady-state activity within 3 h. Deactivation of the catalysts is attributed to carbon deposition catalyzed by acidic sites (24, 25, 29, 30) that are present over Al_2O_3. Acidity of the catalysts was measured by NH_3 chemisorption, which varies in the order **A** (0.23 mmol g^{-1}) < **B** (0.35 mmol g^{-1}) < **C** (0.41 mmol g^{-1}). The higher acidity of catalysts **B** and **C** may be due to the chlorination of the alumina surface by the precursors during catalyst preparation (62). Deactivation occurred to the greatest extent on catalyst **C**. During steady state, catalyst **B** retained ~65% of its initial activity, while the corresponding values for catalysts **A** and **C** were 55% and 25%, respectively. The comparatively lower deactivation/higher

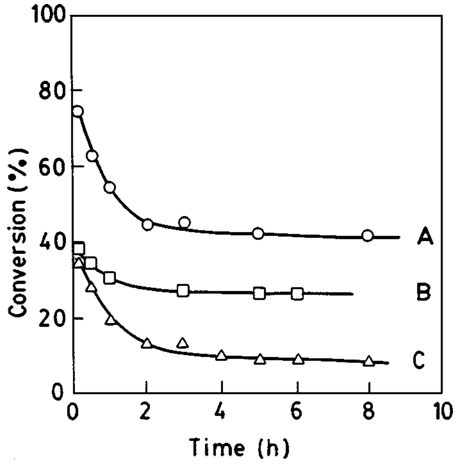

FIG. 4. Time-on-stream study of phenol hydrogenation over 1 wt% Pd/Al_2O_3 catalysts prepared from three different Pd precursors: (**A**) $Pd(OOCCH_3)_2$; (**B**) $PdCl_2$; and (**C**) $Pd(NH_3)_4Cl_2$. Reaction conditions: see Fig. 2.

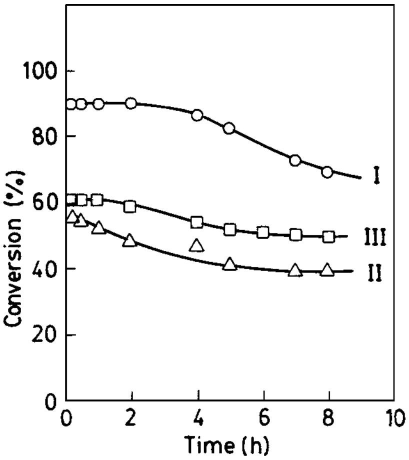

FIG. 5. Time-on-stream study of phenol hydrogenation over 1 wt% Pd/MgO catalysts prepared from three different Pd precursors: (**I**) $Pd(OOCCH_3)_2$; (**II**) $PdCl_2$; and (**III**) $Pd(NH_3)_4Cl_2$. Reaction conditions: see Fig. 2.

stability of catalyst **B**, even though it was more acidic than catalyst **A**, may be due to the presence of residual chlorine in the palladium particles. It is reported that chlorine in the metal particles hinders coke deposition over the metal surface (63).

The deactivation profile of the MgO-based catalysts is shown in Fig. 5. Catalyst **II** deactivates slowly with time from the beginning of the reaction run and attains steady state within 5 h on stream. Catalysts **I** and **III** do not deactivate initially. The zero deactivation period for catalyst **I** during the initial stage is longer than that for catalyst **III**. As mentioned in earlier reports on phenol hydrogenation over supported metal catalysts, deactivation has been attributed to carbon deposition, catalyzed by acidic sites on the surface (24, 25, 29, 30). It has also been reported that deactivation of Pd/MgO during phenol hydrogenation takes place by means of a different reaction mechanism, since MgO is a nonacidic support (30). However, no details are available in the literature. An attempt is made here to account for the deactivation of the Pd/MgO catalyst during the hydrogenation of phenol. Magnesia is a basic material. However, acidic sites can form during catalyst preparation, pretreatment, and even during the reaction. The acidity of the catalysts was measured by NH_3 chemisorption: **I** (nil) < **III** ($0.06\ \mathrm{mmol\ g^{-1}}$) < **II** ($0.07\ \mathrm{mmol\ g^{-1}}$). The aqueous $PdCl_2$ solution (mildly acidified with HCl, pH 3) was used as the precursor of catalyst **II**. The MgO support reacts with HCl and $PdCl_2$ during catalyst preparation and pretreatment, forming $MgCl_2$. Some of the $MgCl_2$ may be left on the surface even after calcination/reduction. This would act as a Lewis acid site to catalyze carbon deposition. Hence, slow and steady deactivation of catalyst **II** starts from the beginning of the reaction run. An ammoniacal $Pd(NH_3)_4Cl_2$ solution, along with NH_4Cl, was the precursor of catalyst **III**. The magnesia surface may become chlorinated by anion exchange during impregnation. Decomposition of the $Pd(NH_3)_4Cl_2$ precursor during drying and calcination also leads to the formation of $MgCl_2$. Thus, some acidic sites are present in catalyst **III**, though their number and strength may be lower than in catalyst **II**. Hence, during time-on-stream, catalyst **III** does not show any deactivation during the initial stage, but it then follows a course similar to that of catalyst **II**. $Pd(OOCCH_3)_2$ was the precursor of catalyst **I**, which readily decomposes to PdO during calcination. There are no acidic sites in the fresh catalyst (confirmed by NH_3 chemisorption). However, during the course of the reaction, acidic sites may form due to dehydroxylation of the MgO surface by the reaction with acidic phenol. Dehydroxylation of MgO catalyzed by Pd may also take place. Alexeev *et al.* observed Pt-catalyzed dehydroxylation of γ-Al_2O_3 (64). Hence, catalyst **I** does not show any deactivation for a longer period at the initial stage of time-on-stream but its behavior is similar to those of catalysts **II** and **III** at a later stage of the reaction. However, deactivation of the catalysts is not severe. After 8 h of reaction, catalysts **I** and **III** retain ~80% while catalyst **II** retains ~70% of the initial activity.

4. CONCLUSIONS

(i) Palladium dispersion in a supported catalyst depends considerably on the precursor as well as on characteristics of the support. $Pd(OOCCH_3)_2$ offers better dispersion of Pd than $PdCl_2$ or $Pd(NH_3)_4Cl_2$ over Al_2O_3 and MgO. Palladium dispersion is higher over MgO-based catalysts compared to Al_2O_3-based catalysts with their respective precursors, which can be attributed to the stronger interaction of Pd with MgO. $Pd(NH_3)_4Cl_2$ leads to lower dispersion of Pd, probably due to the presence of inherent NH_3 (a reducing agent) and facile surface mobility of the precursor.

(ii) All of the catalysts originating from chlorinated precursors (either $PdCl_2$ or $Pd(NH_3)_4Cl_2$) retain a considerable amount of chlorine on the support even after calcination/reduction. In addition, Pd particles in Pd/Al_2O_3, originating from $PdCl_2$, also retain some chlorine after the same pretreatment. The absence of residual chlorine in the Pd particles in the other catalysts originating from chlorinated precursors was discussed.

(iii) Phenol hydrogenation activity over the catalysts is a direct function of the available palladium area. However, residual chlorine in the metal particles or at the metal–support interface reduces activity.

(iv) Pd precursors do not have a significant influence on the product distribution of phenol hydrogenation. Al_2O_3-based catalysts are totally selective for cyclohexanone production. MgO-based catalysts produce cyclohexanone, the main product, as well as cyclohexanol, a minor product. Correlations between phenol conversion and product selectivity/yield reveal that changes in product selectivity may not be merely due to a change in the overall conversion, and one product does not form at the expense of another. Formation of cyclohexanol along with the main product cyclohexanone is attributed to the strong basicity of MgO. A fraction of the strongly bound phenol, in the form of phenolate, undergoes complete hydrogenation to cyclohexanol before desorption.

(v) Acidic sites present over Al_2O_3 causes severe deactivation of the Pd/Al_2O_3 catalysts, while MgO-based catalysts show strong resistence to deactivation.

ACKNOWLEDGMENTS

We are grateful to the reviewers for valuable comments and helpful suggestions. Financial support by UGC, New Delhi (SRF), is gratefully acknowledged.

REFERENCES

1. Karpinski, Z., *Adv. Catal.* **37**, 45 (1990).
2. Maier, W. F., *in* "Catalysis of Organic Reactions" (P. N. Rylander, H. Greenfield, and R. L. Augustine, Eds.), p. 233, Dekker, New York, 1988.
3. Zou, W., and Gonzalez, R. D., *Catal. Lett.* **12**, 73 (1992).
4. Pitchai, R., Wong, S. S., Takahashi, N., Butt, J. B., Burwell, R. L., Jr., and Cohen, J. B., *J. Catal.* **94**, 478 (1985).
5. Bonivardi, A. L., and Baltanas, M. A., *J. Catal.* **125**, 243 (1990).
6. Bonivardi, A. L., and Baltanas, M. A., *J. Catal.* **138**, 500 (1992).
7. Tessier, D., Rakai, A., and Bozon-Verduraz, F., *J. Chem. Soc., Faraday Trans.* **88**, 741 (1992).
8. Rakai, A., Tessier, D., and Bozon-Verduraz, F., *New J. Chem.* **16**, 8 (1992).
9. Lomot, D., Juszczyk, W., Karpinski, Z., and Bozon-Verduraz, F., *J. Chem. Soc., Faraday Trans.* **93**, 2015 (1997).
10. Ali, S. H., and Goodwin, J. G., Jr., *J. Catal.* **176**, 3 (1998).
11. Sepulveda, J., and Figoli, N., *React. Kinet. Catal. Lett.* **53**, 155 (1994).
12. Sales, E. A., Bugli, G., Ensuque, A., Mendes, M. de J., and Bozon-Verduraz, F., *Phys. Chem. Chem. Phys.* **1**, 491 (1999).
13. Kepinski, L., Wolcyrz, M., and Okal, J., *J. Chem. Soc., Faraday Trans.* **91**, 507 (1995).
14. Contescu, C., Macovei, D., Craiu, C., Teodorescu, C., and Schwarz, J. A., *Langmuir* **11**, 2031 (1995).
15. Shen, Y., Wang, S., and Huang, K., *Appl. Catal.* **57**, 55 (1990).
16. Deligianni, H., Mieville, R. L., and Peri, J. B., *J. Catal.* **95**, 465 (1985).
17. Kelly, K. P., Tatsumi, T., Uematsu, T., Driscoll, D. J., and Lunsford, J. H., *J. Catal.* **101**, 396 (1986).
18. Bozon-Verduraz, F., Omar, A., Escard, J., and Pontvianne, B., *J. Catal.* **53**, 126 (1978).
19. Oberender, H., Shaefer, H., Trimm, D., Baltz, H., Blume, H., Lanau, J., and Meye, H., British Patent 1 332211, 1973.
20. Fisher, W. B., and Van Peppen, J. F., U.S. Patent 4 162267, 1978.
21. Ulmer, S., Harry, E., and Chuen, Y., U.S. Patent 4 203923, 1980.
22. Dodgson, I., Griffin, K., Barberis, G., Pignataro, F., and Tauszik, G., *Chem. Ind.* 830 (1989).
23. Narayanan, S., and Krishna, K., *Appl. Catal. A: General* **147**, L253 (1996).
24. Mahata, N., Raghavan, K. V., and Vishwanathan, V., *Appl. Catal. A: General* **182**, 183 (1999).
25. Mahata, N., and Vishwanathan, V., *Catal. Today* **49**, 65 (1999).
26. Mahata, N., and Vishwanathan, V., *J. Mol. Catal. A: Chemical* **120**, 267 (1997).
27. Talukdar, A. K., Bhattacharyya, K. G., and Sivasanker, S., *Appl. Catal. A: General* **96**, 229 (1993).
28. Chen, Y. Z., Liaw, C. W., and Lee, L. I., *Appl. Catal. A: General* **177**, 1 (1999).
29. Neri, G., Visco, A. M., Donato, A., Milone, C., Malentacchi, M., and Gubitosa, G., *Appl. Catal. A: General* **110**, 49 (1994).
30. Galvagno, S., Donato, A., Neri, G., and Pietropaolo, R., *J. Chem. Tech. Biotechnol.* **51**, 145 (1991).
31. Higashijima, M., and Nishimura, S., *Bull. Chem. Soc. Jpn.* **65**, 2955 (1992).
32. Gonzalez-Velasco, J. R., Gutierrez-Ortiz, J. I., Gonzalez-Marcos, J. A., and Romero, A., *React. Kinet. Catal. Lett.* **32**, 505 (1986).
33. Mahata, N., and Vishwanathan, V., *Indian J. Chem.* **37A**, 652 (1998).
34. Srinivas, S. T., and Rao, P. K., *J. Chem. Soc., Chem. Commun.* 33 (1993).
35. Srinivas, S. T., Lakshmi, L. J., and Rao, P. K., *Appl. Catal. A: General* **110**, 167 (1994).
36. Smith, H. A., and Stump, B. L., *J. Am. Chem. Soc.* **83**, 2739 (1961).
37. Gutierrez-Ortiz, M. A., Castano, A., Gonzalez-Marcos, M. P., Gutierrez-Ortiz, J. I., and Gonzalez-Velasco, J. R., *Ind. Eng. Chem. Res.* **33**, 2571 (1994).
38. Hancil, V., and Beranek, L., *Chem. Eng. Sci.* **25**, 1121 (1970).
39. Shin, E.-J., and Keane, M. A., *J. Catal.* **173**, 450 (1998).
40. Narayanan, S., and Sreekanth, G., *Indian J. Technol.* **31**, 507 (1993).
41. Gonzo, E. E., and Boudart, M., *J. Catal.* **52**, 462 (1978).
42. Sarkany, A., Zsoldos, Z., Furlong, B., Hightower, J. W., and Guczi, L., *J. Catal.* **141**, 566 (1993).
43. Vannice, M. A., Wang, S.- Y., and Moon, S. H., *J. Catal.* **71**, 152 (1981).
44. Nag, N. K., *Catal. Lett.* **24**, 37 (1994).
45. Fan, L., and Fujimoto, K., *Bull. Chem. Soc. Jpn.* **67**, 1773 (1994).
46. Anderson, J. R., "Structure of Metallic Catalysts." Academic Press, London, 1975.
47. Zhou, Y., Wood, M. C., and Winograd, N., *J. Catal.* **146**, 82 (1994).
48. Johnston, P., and Joyner, R. W., *J. Chem. Soc., Faraday Trans.* **89**, 863 (1993).
49. Elding, L. I., and Olsson, L. F., *J. Phys. Chem.* **82**, 69 (1978).
50. Stolz, C., Sauvage, A., Massiani, P., and Kramer, R., *Appl. Catal. A: General* **167**, 113 (1998).
51. Brown, G. E., Jr., Henrich, V. E., Casey, W. H., Clark, D. L., Eggleston, C., Felmy, A., Goodman, D. W., Gratzel, M., Maciel, G., McCarthy, M. I., Nealson, K. H., Sverjensky, D. A., Toney, M. F., and Zachara, J. M., *Chem. Rev.* **99**, 77 (1999).
52. Jiang, Y., Decker, S., Mohs, C., and Klabunde, K. J., *J. Catal.* **180**, 24 (1998).
53. Babaeva, M. A., Bystrov, D. S., Kovalgin, A. Y., and Tsyganenko, A. A., *J. Catal.* **123**, 396 (1990).
54. Zecchina, A., Coluccia, S., Spoto, G., Scarano, D., and Marchese, L., *J. Chem. Soc., Faraday Trans.* **86**, 703 (1990).
55. Vogel, W., Knozinger, H., Carvile, B. T., Sachtler, W. M. H., and Zhang, Z. C., *J. Phys. Chem. B* **102**, 1750 (1998).
56. Homeyer, S. T., and Sachtler, W. M. H., *J. Catal.* **117**, 91 (1989).
57. Herz, R. K., and Marin, S. P., *J. Catal.* **65**, 281 (1980).
58. Hoang-Van, C., Kachaya, Y., Teichner, S. J., Arnaud, Y., and Dalmon, J. A., *Appl. Catal.* **46**, 281 (1989).
59. Lopez, N., and Illas, F., *J. Phys. Chem. B* **102**, 1430 (1998).
60. Ferrari, A. M., and Pacchioni, G., *J. Phys. Chem.* **100**, 9032 (1996).
61. Kondarides, D. I., and Verykios, X. E., *J. Catal.* **174**, 52 (1998).
62. Chambers, A., and Baker, R. T. K., *J. Phys. Chem. B* **101**, 1621 (1997).
63. Pieck, C. L., Marecot, P., Parera, J. M., and Barbier, J., *Appl. Catal. A: General* **126**, 153 (1995).
64. Alexeev, O., Kim, D.-W., Graham, G. W., Shelef, M., and Gates, B. C., *J. Catal.* **185**, 170 (1999).